# Static, continuous and dynamic calibration of force transducers: A comparative study on a low-force strain-gauge measuring device

Measurement: Sensors xxx (xxxx) xxx

Contents lists available at ScienceDirect

Measurement: Sensors

journal homepage: www.sciencedirect.com/journal/measurement-sensors

# Static, continuous and dynamic calibration of force transducers: A comparative study on a low-force strain-gauge measuring device

ARTICLE INFO

*Keywords:*
Force transducer
Force calibration
Static
Continuous
Dynamic

ABSTRACT

Current ISO 376 standard focuses on static calibration of force transducers, overlooking time and frequency influences, crucial in real-world applications such as automotive, aerospace, and healthcare, where mechanical and materials testing is essential for product quality and safety. As a result, novel calibration guidelines have been proposed to extend calibration to continuous and dynamic loading conditions. The paper examines the calibration results of a 200 N high-precision strain-gauge force transducer under static, continuous, and dynamic conditions. While sensitivities across these conditions are generally compatible, uncertainties in continuous and dynamic calibrations are notably higher, which could impact material testing and related applications. If continuous and dynamic sensitivity uncertainties dropped to the static uncertainty level, compatibility would be compromised because of significant differences between the three. It's unclear whether these discrepancies arise mainly from the intrinsic characteristics of the transducer in continuous dynamic conditions or from the inability to reach the transducer capacity force values during dynamic calibration.

## 1. Introduction

Mechanical and materials testing are crucial across a spectrum of industries, including automotive, aerospace, and healthcare, where product quality and safety are paramount. However, conventional force measurement techniques in these sectors often fail to account for the dynamic nature of real-world applications, disregarding factors such as time and frequency. This oversight can lead to a lack of metrological traceability, undermining the reliability of test results. While ISO 376 [1] currently provides guidelines for static calibration of force transducers, the pervasive use of these transducers in material testing machines necessitates a broader approach encompassing continuous and dynamic loading conditions. In response, recent advancements in calibration methodologies have led to the development of novel guidelines tailored to these requirements, for example, DKD-R 3-9 [2] for the continuous calibration of force transducers according to the comparison method, and DKD-R 3-10 (Sheet 2) [3] for the dynamic calibration of force transducers according to the sinusoidal method. This paper contributes to this evolving field by conducting a comparative analysis of the calibration process for a specific high-precision strain-gauge force transducer with a 200 N capacity, examining its performance under static, continuous, and dynamic loading conditions in compression. Through meticulous examination and comparison of calibration results across these varied conditions, the study aims to show any discrepancies and identify compatibilities, thereby enhancing understanding and improving the accuracy of force measurement in practical applications.

## 2. Methods and procedures

### 2.1. Transducer under test

Measurements are carried on a 200 N strain gauge force transducer produced by HBK (TOP-Z30A), as shown in Fig. 1. This force transducer measures small tensile and compressive forces with high accuracy (Class 00 according to ISO 376), thus is often used as a reference transducer in calibration machines, or as transfer standard for machine calibration according to ISO 7500-1 [4]. The transducer is connected to a NI-9237 measuring amplifier (Fig. 2), with a resolution of 0.000 001 mV/V, through a 3 m 6-wires-to-LAN cable. This amplifier includes all the signal conditioning required to power and measure up to four 6-wires bridge-based sensors simultaneously and provides strain or load measurements with zero interchannel phase delay. The maximum sampling rate is 50 kHz. The module is connected to the PC through a NI-9162 USB carrier and a USB cable. Acquired data are managed by LabView© software.

### 2.2. Static calibration according to ISO 376

Static calibration in compression of the selected transducer is performed according to ISO 376 using the INRiM 2.5 kN deadweight force standard machine (Fig. 3). The Calibration and Measurement Capability (CMC) relative expanded uncertainty declared for this machine is 20 ppm.

Ten equally-spaced forces are consecutively generated from 20 N to 200 N in loading and unloading conditions with dwell times of over 30 s per step, at three rotational positions (0°, 120° and 240°) as required by the standard. A 0.1 Hz Bessel filter setting is used to minimise fluctuations in the signal. The determination of transducer sensitivity $S_{stat}$ and

https://doi.org/10.1016/j.measen.2024.101337


**Fig. 1.** The 200 N strain gauge force transducer (HBK TOP-Z30A).

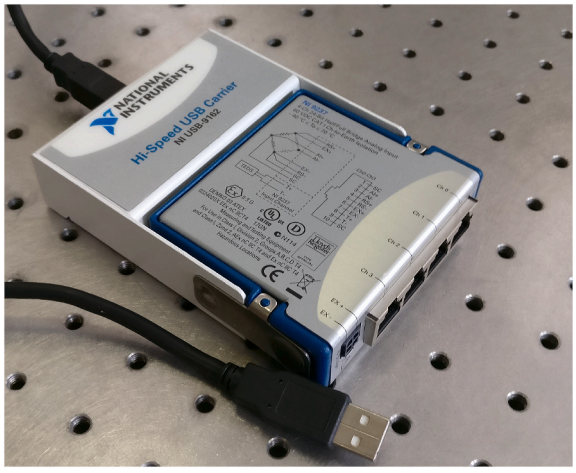


**Fig. 2.** NI-9237 measuring amplifier.

characteristic properties such as repeatability ($b$'), reproducibility ($b$), resolution, hysteresis ($\nu$), return to zero and total relative expanded uncertainty $W(S_{stat})$ is carried out for every 10 % force step from 20 N to 200 N. The interpolation error is not evaluated since the comparison is carried out for each force step (Case B of ISO 376). An additional calibration is performed according to ISO 376 at specific forces from 1 N to 20 N, with steps of 1 N from 1 N to 10 N and steps of 2 N from 10 N to 20 N, to evaluate sensitivity also at very low forces.

### 2.3. Continuous calibration according to DKD-R 3-9

Continuous calibration in compression is carried out according to DKD-R 3-9 using the INRiM 1 kN continuous force calibration machine, shown in Fig. 4, capable of generating continuous forces via a stepper motor (Orientalmotor α-GRADE AR Series - AR HM 40093E 24DC), connected to a screw through a gearbox. It was designed and used for testing polymers [5], but, at a later time, also characterized to be suitable for continuous force calibration.

Reference force is measured by a 1 kN high precision force transducer (HBM Z3H3) located at the bottom of the machine and connected to the above-mentioned NI-9267 module. This reference transducer was previously characterised according to DKD-R 3-9 Annex A [2] to evaluate the best measurement capability of the force calibration machine with reference force transducer system in continuous operation. Correction factors used in the linear product model related to various parameters (e.g. long-term drift, hysteresis, transfer transducer, etc.) and associated uncertainties, as deeply described in DKD-R 3-9 Annex A.4.2 [2], were found. Relative expanded uncertainty of generated

**Fig. 3.** INRiM 2.5 kN deadweight force standard machine.

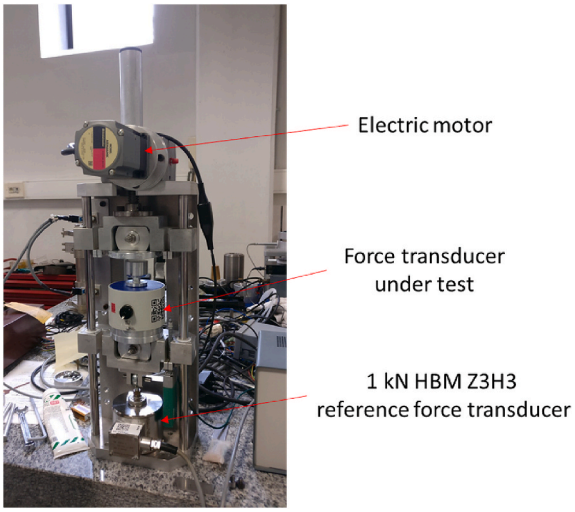


**Fig. 4.** The INRiM 1 kN continuous force calibration machine.

continuous reference forces $W_{cont}$ is equal to 0.27 %.

The test sequence is carried out up to a nominal load of 200 N in compression mode, according to DKD-R 3–9 guidelines. Calibration is performed at a period of 120 s for the load to reach 100 % of the specified nominal load. Evaluation is conducted with the ramp force-time profile. Data from both transducers are simultaneously acquired and synchronised with a sample rate of 25 Hz and a 0.1 Hz Bessel filter. A table of values is generated for increasing and decreasing forces. The determination of transducer sensitivity and characteristic properties such as repeatability, hysteresis, reproducibility and zero error follows the same methodology as static investigations, for ten force steps from

20 N to 200 N. Considerations for temperature influence are not taken into account since all calibration measurements are performed in controlled environmental conditions (i.e., 21.0 ± 0.5 °C).

### 2.4. Dynamic calibration according to DKD-R 3-10

Dynamic calibration is carried out following guideline DKD-R 3-10 (Sheet 2) by using INRiM primary vibration calibration system (Figs. 5 and 6) [6]. This is composed of a vibrating table, PCB model TMS 2075E, capable of oscillating with a maximum frequency of 6000 Hz, and a Polytec OFV-5000 laser interferometer used for mass acceleration measurement, necessary for dynamic force calculation. A set of cylindrical weights of 207.24 g, 313.07 g, 419.02 g and 525.41 g are adopted as loading masses. For the study of resonance phenomena, the acceleration of the vibrating table is also measured via a single-sided accelerometer. The components used for data acquisition are PCB 482C Series signal conditioner, National Instruments NI 4431, NI 9162 and NI 9237 data cards. Data are acquired with a 5 kHz sampling rate. The amplitude and frequency of oscillation of the vibrating table are generated with LabView© software. The measured data are analysed with Matlab© and Microsoft Excel©.

For the calibration, it is necessary to measure the output of the force transducer, and the accelerations of the loading mass and the vibrating table. In fact, according to DKD-R 3-10 [3], the desired calibration quantity, namely the dynamic sensitivity $S_{\mathrm{dyn}}$, is the frequency-dependent ratio of the force transducer output $U_{\mathrm{f}}$ (in mV/V) to the acting dynamic force $F_{\mathrm{dyn}}$, given by multiplying the sum of the loading mass $m_{\mathrm{t}}$ and internal mass of the transducer $m_{\mathrm{i}}$ by the acceleration experienced by the loading mass, $a_{\mathrm{t}}$, according to (1).

$$S_{\mathrm{dyn}} = \frac{U_{\mathrm{f}}}{(m_t + m_{\mathrm{i}})a_t} \,. \tag{1}$$

This model applies to rigid bodies. In an elastic structure, however, the individual mass points experience – to a small extent – different accelerations in the vertical direction. The acceleration which in practice is measured on the upper side of the load mass by means of a laser vibrometer slightly differs from the amplitude generated by the vibration base.

To take into account the elastic behaviour, which is visible around the resonant frequency of the mass-spring system, dynamic sensitivity derived from the solution of differential equations of the motion, can be approximated to

$$S_{\mathrm{dyn,fit}} = p_1\left(1 - p_2\omega^2\right). \tag{2}$$

where $p_1$ and $p_2$ are parameters found through a linear regression model of the experimental dynamic sensitivities as a function of frequency found according to (1).

Prior to calibration measurements, the internal (inertial) mass of the transducer $m_{\mathrm{i}}$ is evaluated by applying the methodology described in DKD-R 3-10 (§3.3.1) [3]. An internal mass $m_{\mathrm{i}}$ equal to 122 g is found.

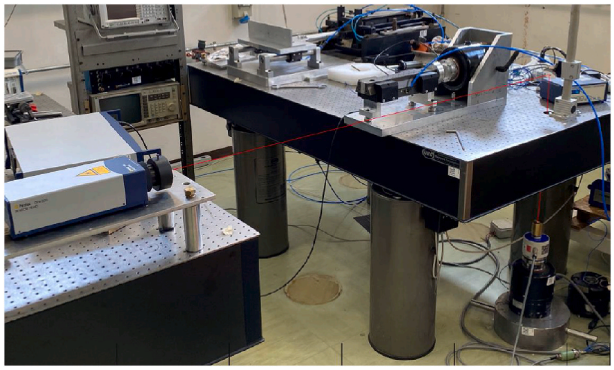

**Fig. 5.** INRiM dynamic force and vibration calibration system.

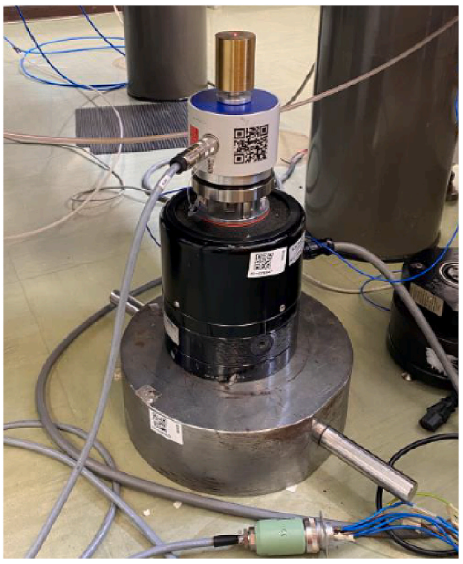

**Fig. 6.** Force transducer with screwed a cylindrical loading mass, mounted on the vibrating table.

Actual calibration measurements are then performed with all available test masses. 90 sinusoidal forces are generated consecutively for 30 seconds each, ranging from 10 Hz to 1000 Hz at a nearly-constant amplitude of 2 m $s^{-2}$; therefore, with the selected weights and the internal mass, generated dynamic force amplitudes range from around 0.7 N–1.3 N, i.e., from around 0.3 %–0.6 % of the transducer capacity. Adding the static force generated by the weights, maximum compressive forces from 2.7 N to 6.4 N, i.e., from 1.3 % to 3.2 % of the transducer capacity, are reached.

The calculation of the uncertainties for individual dynamic sensitivity measurements in frequency is carried out following the GUM guide JCGM 100:2008 [7] applied to (1). Uncertainty contributions of input parameters of (1) are mainly due to the adopted instrumentation and repeated measurements. Then, a Monte Carlo method is used to propagate these uncertainties on the dynamic sensitivity model in (2), in accordance with GUM guide JCGM 101:2008 [8] and DKD-R 3-10 (§3.4) [3].

## 3. Results and discussion

### 3.1. Static calibration results

The results of the measurements carried out according to ISO 376 are given in Table 1. Data fulfil Class 00 requirements from 9 N to 200 N, and Class 05 from 1 N to 8 N. Sensitivity values are constant and consistent for the whole tested force range (see Table 2).

**Table 1**
Results according to ISO 376 in compression from 20 N to 200 N.

| $F$/N | $S_{\mathrm{stat}}$/(mV/V)/N | $b$/% | $b'$/% | $\nu$/% | $W(S_{\mathrm{stat}})$/% |
|---|---|---|---|---|---|
| 20 | 0.010 001 | 0.010 | 0.000 | 0.010 | 0.010 |
| 40 | 0.010 001 | 0.002 | 0.000 | 0.002 | 0.004 |
| 60 | 0.010 001 | 0.002 | 0.000 | 0.005 | 0.004 |
| 80 | 0.010 001 | 0.001 | 0.000 | 0.004 | 0.003 |
| 100 | 0.010 000 | 0.002 | 0.000 | 0.001 | 0.003 |
| 120 | 0.010 001 | 0.001 | 0.000 | 0.004 | 0.003 |
| 140 | 0.010 001 | 0.001 | 0.000 | 0.003 | 0.003 |
| 160 | 0.010 001 | 0.001 | 0.000 | 0.004 | 0.003 |
| 180 | 0.010 000 | 0.004 | 0.000 | 0.001 | 0.004 |
| 200 | 0.010 000 | 0.000 | 0.000 | /// | 0.002 |

**Table 2**
Results according to ISO 376 in compression from 1 N to 20 N.

| $F$/N | $S_{stat}$/(mV/V)/N | $b$/% | $b'$/% | $\nu$/% | $W(S_{stat})$/% |
|---|---|---|---|---|---|
| 1 | 0.010 001 | 0.069 | 0.037 | 0.002 | 0.059 |
| 2 | 0.010 000 | 0.099 | 0.042 | 0.050 | 0.077 |
| 3 | 0.010 000 | 0.073 | 0.041 | 0.008 | 0.064 |
| 4 | 0.010 002 | 0.070 | 0.004 | 0.035 | 0.043 |
| 5 | 0.010 002 | 0.077 | 0.046 | 0.007 | 0.073 |
| 6 | 0.010 002 | 0.073 | 0.034 | 0.012 | 0.058 |
| 7 | 0.010 002 | 0.079 | 0.023 | 0.003 | 0.053 |
| 8 | 0.010 002 | 0.064 | 0.005 | 0.010 | 0.038 |
| 9 | 0.010 002 | 0.049 | 0.011 | 0.001 | 0.032 |
| 10 | 0.010 001 | 0.042 | 0.016 | 0.008 | 0.031 |
| 12 | 0.010 001 | 0.041 | 0.011 | 0.006 | 0.030 |
| 14 | 0.010 001 | 0.032 | 0.010 | 0.004 | 0.024 |
| 16 | 0.010 001 | 0.022 | 0.014 | 0.007 | 0.022 |
| 18 | 0.010 001 | 0.032 | 0.009 | 0.001 | 0.023 |
| 20 | 0.010 001 | 0.018 | 0.005 | /// | 0.013 |

### 3.2. Continuous calibration results

The results obtained in compression are listed in Table 3 for the ramp force-time profile.

Sensitivities are almost linear, except at 40 N, 100 N and 200 N, where values deviate a little from the expected trend found for static sensitivities. Uncertainties increase considerably not only because of the higher standard uncertainty of the generated continuous force, which, as described in the previous section, is equal to 0.135 %, but mainly because of the reversibility, which, if compared with the static case, shows significantly higher values. This may be due not only to the behaviour of the transducer under continuous loading but also to how the reference transducer is connected to the transducer under calibration. A similar finding was found in Ref. [9] for a piezoelectric transducer.

### 3.3. Dynamic calibration results

Calibration results, in terms of sensitivity, in dynamic conditions are shown in Fig. 7 as a function of frequency and loading mass.

As hypothesised, results confirm that dynamic sensitivity follows a parabolic decreasing trend as a function of frequency. From the graph, it is possible to observe some irregularities due to resonance phenomena of the connecting parts, rather than around the resonance frequencies of the mass-spring system. These were calculated from the ratio between the acceleration of the loading mass $a_t$ and the acceleration of the vibrating table $a_b$ (Fig. 8).

As expected, the resonance frequency is higher when the loading mass is smaller. Anyway, even from these graphs it is possible to see the small alterations at the same frequencies as in Fig. 7 due mainly to the resonances of the connecting organs. These typically resonate at frequencies higher than the resonance frequencies of the mass-spring system and are minimized by adopting a less rigid connection.

Relative expanded uncertainties $W(S_{dyn})$ are in the order of 0.3 %, calculated considering the uncertainties associated with the loading masses $m_t$, the output signals of the force transducer $U_f$, the acceleration values measured by the laser interferometer $a_t$ and the calculation of the internal mass $m_i$.

Subsequently, the linear regression described above is carried out to find $p_1$ and $p_2$ values, for the four loading masses. Results are shown in Table 4.

$p_1$ coefficients are very close to the static sensitivity for all loading masses. On the other hand, $p_2$ coefficients are different depending on the connected loading mass. Resulting fitted dynamic sensitivity curves are shown in Fig. 9.

Comparison of experimental and model curves is shown in Fig. 10 for the 528.9 g loading mass. The alteration of the experimental curve due to the resonant frequency of connection adapters disappears in the fitted curve.

**Table 3**
Results for continuous loading according to DKD-R 3-9 with the ramp force time profile in compression mode.

| $F$/N | $S_{cont}$/(mV/V)/N | $w_{rep}$/% | $w_{rot}$/% | $w_{rev}$/% | $W(S_{cont})$/% |
|---|---|---|---|---|---|
| 20 | 0.00998 | 0.009 | 0.013 | 0.456 | 0.95 |
| 40 | 0.00988 | 0.002 | 0.007 | 0.222 | 0.52 |
| 60 | 0.01001 | 0.000 | 0.014 | 0.219 | 0.52 |
| 80 | 0.00999 | 0.001 | 0.013 | 0.341 | 0.73 |
| 100 | 0.00992 | 0.001 | 0.006 | 0.427 | 0.90 |
| 120 | 0.00999 | 0.001 | 0.004 | 0.535 | 1.10 |
| 140 | 0.00999 | 0.000 | 0.005 | 0.505 | 1.05 |
| 160 | 0.00999 | 0.000 | 0.006 | 0.435 | 0.91 |
| 180 | 0.01000 | 0.000 | 0.007 | 0.362 | 0.77 |
| 200 | 0.01005 | 0.000 | 0.011 | /// | 0.27 |

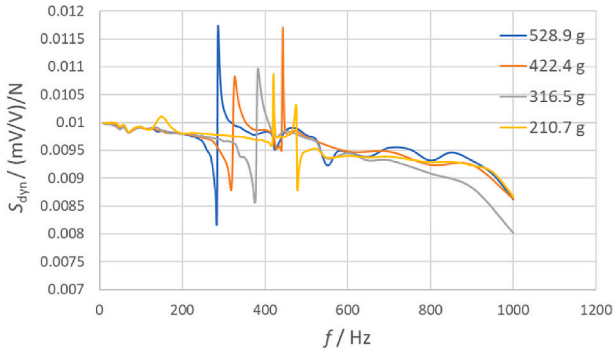


**Fig. 7.** Dynamic sensitivity as function of frequency and loading mass.

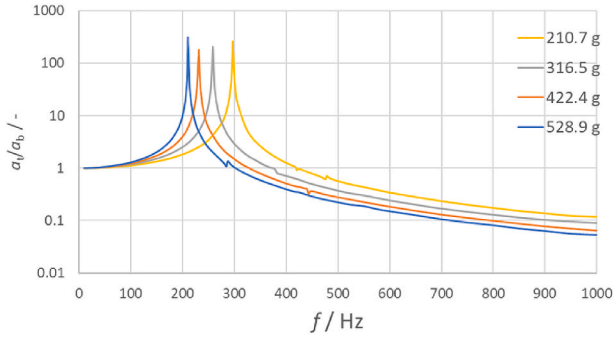


**Fig. 8.** Ratio between the acceleration of the loading mass $a_t$ and the acceleration of the vibrating table $a_b$, to evaluate resonant frequency of the mass-spring systems for different loading masses.

**Table 4**
Values of $p_1$ and $p_2$ coefficients according to (2) as a function of the loading mass.

| $m_t$/g | $p_1$/(mV/V)/N | $p_2$/s$^2$ |
|---|---|---|
| 210.67 | 0.0099 1164 | $2.6958 \times 10^{-9}$ |
| 316.46 | 0.0099 3533 | $3.4029 \times 10^{-9}$ |
| 422.40 | 0.0099 3682 | $2.2692 \times 10^{-9}$ |
| 528.88 | 0.0099 5425 | $2.4844 \times 10^{-9}$ |

Relative expanded uncertainties $W(S_{dyn,fit})$ increase as function of frequency for all loading masses from around 1 % to around 7÷8 %, as shown in Fig. 11.

As described above, they are evaluated using a Monte Carlo method for uncertainty propagation [10], starting from the uncertainty of input quantities of the linear regression (mainly $S_{dyn}$, rather than $\omega$). To these, the standard uncertainty from ordinary least squares (OLS) for linear

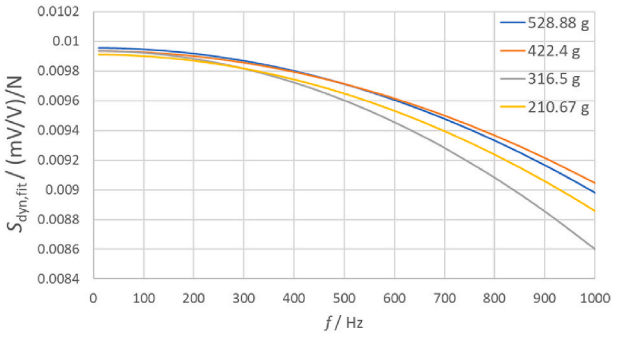


**Fig. 9.** Fitted dynamic sensitivity curves $S_{dyn,fit}$.

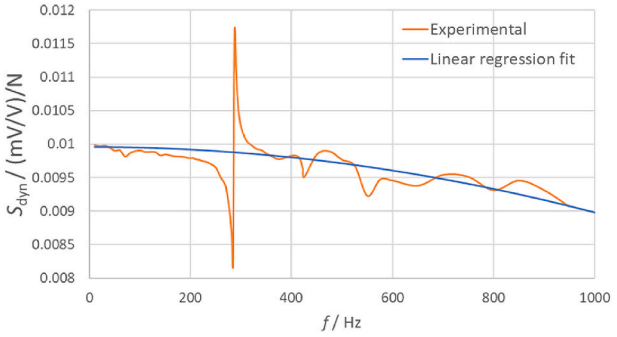


**Fig. 10.** Comparison between $S_{dyn}$ and $S_{dyn,fit}$ curves for the 528.9 g loading mass.

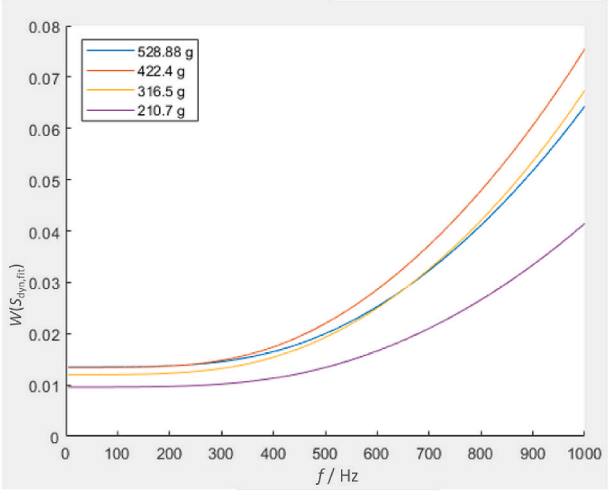


**Fig. 11.** Relative expanded uncertainties associated with dynamic sensitivity arising from linear regression fit.

regression is included. The latter is one order of magnitude larger than the Monte Carlo ones, mainly due to the higher dispersion of experimental data around the resonant frequency of the connection adapters, as previously shown in Fig. 7.

### 3.4. Comparison of the results of different calibration methods

First of all, it is worth comparing static and continuous results at common force steps from 20 N to 200 N. In Fig. 12, results from the two loading conditions are plotted together with expanded uncertainties. As shown in Sections 3.1 and 3.2, uncertainties associated with static sensitivities are much lower than continuous ones. Anyway, values are

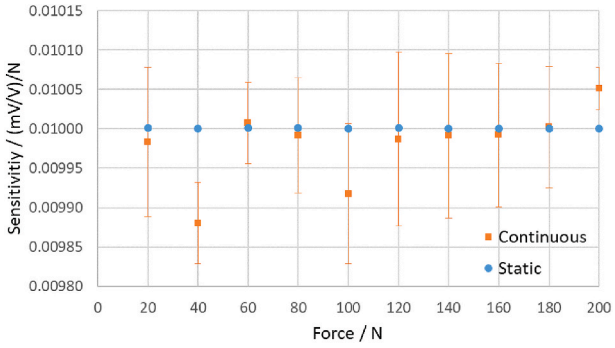


**Fig. 12.** Comparison between static and continuous calibration results in terms of transducer sensitivity as function of applied load.

compatible except for sensitivities at 40 N and 200 N, where continuous calibration values deviate from the expected linear trend. This happens also at 100 N, as shown in Section 3.2, but in this case its uncertainty compensates such discrepancy. Possible causes of such discrepancies might be due to oscillations in the identification of zero values or defects in the mechanical connections between reference and under-calibration transducers.

To compare static and continuous calibration results with dynamic ones, the mean static $S_{stat,mean}$ and continuous sensitivities $S_{cont,mean}$ are calculated. These are equal to 0.010 001 (mV/V)/N and 0.009 980 (mV/V)/N, respectively. The associated expanded uncertainties are calculated as two times the square root of the sum of the squares of the mean standard uncertainty of all force steps and the standard deviation of the sensitivities of all force steps [10,11]. Relevant relative expanded uncertainties $W(S_{stat,mean})$ and $W(S_{cont,mean})$, in this way, are equal to 0.030 % and 0.772 %, respectively.

Comparison results are shown in Fig. 13. It can be seen that static and continuous sensitivities are slightly higher than dynamic ones, in particular at low frequencies, while at increasing frequencies dynamic sensitivities diverge. It is also important to underline that dynamic sensitivities are reported as function of frequency while static and continuous ones represent an equivalent frequency $f = 0$ Hz. For this reason, it might be more significant to compare the results in a restricted low frequency range (up to 100 Hz), shown in Fig. 14, since at higher frequencies dynamic sensitivities significantly decrease. In this figure, dotted lines corresponding to lower and upper limits of mean static and continuous sensitivities with associated expanded uncertainty are also plotted to verify compatibility. Uncertainties of dynamic sensitivities, in the order of 1 % below 100 Hz, are not plotted to keep the figure clearer.

In this way, compatible results are found between all sensitivities despite different loading conditions. However, in this case, compatibility is highly dependent on the declared uncertainties. If dynamic and continuous sensitivity uncertainty decreased down to static sensitivity uncertainty level, compatibility would be compromised, since

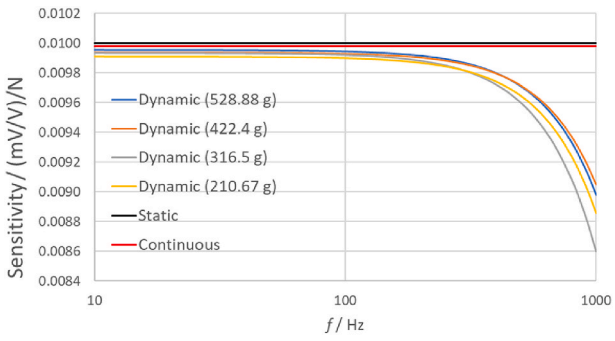


**Fig. 13.** Comparison between static, continuous and dynamic calibration sensitivities.

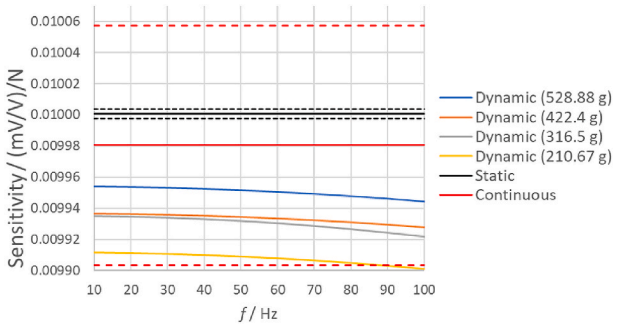


**Fig. 14.** Comparison between static, continuous and dynamic calibration sensitivities up to 100 Hz. Dotted lines correspond to lower and upper limits of mean static and continuous sensitivities with associated expanded uncertainty.

differences are rather high compared to static sensitivity. In particular, by taking static sensitivity as a reference, continuous one is the closest while dynamic sensitivities become more distant as the loading mass decreases, similarly to Ref. [12]. This could mean that, the farther we move away from the transducer capacity, the farther the dynamic sensitivity moves away from the static value. However, since the dynamic sensitivities at higher forces close to transducer capacity remain unknown, doubts remain about the actual effectiveness of this dynamic calibration method, which inevitably leads to problems although conceptually and metrologically correct. In fact, when fatigue material testing machines are verified and calibrated [13], the transfer transducer is dynamically used up to its maximum capacity but these force values cannot be reached during dynamic calibration (especially with high-capacity transducers).

The same can be stated for the uncertainties. In continuous and dynamic conditions, where uncertainties are orders of magnitude higher than static ones, it is not evident whether this is due to the intrinsic characteristic of the transducer or due to proposed calibration methods or systems. Therefore, attention must be paid to all these aspects before the standardisation of the proposed continuous and dynamic methods.

## 4. Conclusions

This paper provides insights into the calibration outcomes of a 200 N high-precision strain-gauge force transducer under various conditions. It highlights that while sensitivities remain generally consistent across static, continuous, and dynamic calibrations, uncertainties are orders of magnitude higher in continuous and dynamic scenarios, raising questions about whether this is caused by intrinsic transducer characteristics or by the calibration methods/systems employed. Furthermore, if dynamic and continuous sensitivity uncertainties were reduced to static uncertainty levels, compatibility would be compromised due to significant differences. These discrepancies, beyond being caused by strain-gauge force transducer altered behaviour under continuous or dynamic conditions, might also be due to the inability to generate force values equivalent to the transducer capacity during dynamic calibration. These findings underscore the need for caution regarding the actual effectiveness of the suggested continuous and dynamic calibration methods, despite their conceptual and metrological correctness, because they could have potential implications for material testing applications.

## Funding statement

This work was supported by EURAMET [18SIB08 ComTraForce project funded by the EMPIR programme].

## References

[1] ISO 376, Metallic Materials — Calibration of Force-Proving Instruments Used for the Verification of Uniaxial Testing Machines, 2011.
[2] DKD-R 3-9, Continuous Calibration of Force Transducers According to the Comparison Method, 2020.
[3] DKD-R 3-10, (Sheet 2) — Dynamic Calibration of Force Transducers According to the Sinusoidal Method, 2019.
[4] ISO 7500-1, Verification of Static Uniaxial Testing Machines —Part 1: Tension/compression Testing Machines — Calibration and Verification of the Force-Measuring System, 2018.
[5] A. Schiavi, A. Prato, Evidences of non-linear short-term stress relaxation in polymers, Polym. Test. 59 (2017) 220–229, https://doi.org/10.1016/j.polymertesting.2017.01.030.
[6] A. Prato, F. Mazzoleni, A. Schiavi, Metrological traceability for digital sensors in smart manufacturing: calibration of MEMS accelerometers and microphones at INRiM, 2019 II Workshop on Metrology for Industry 4.0 and IoT (MetroInd4.0&IoT). https://doi.org/10.1109/METROI4.2019.8792906, 2019.
[7] JCGM 100, Evaluation of Measurement Data — Guide to the Expression of Uncertainty in Measurement (GUM), Joint Committee for Guides in Metrology, Sèvres, France, 2008.
[8] JCGM 101, Evaluation of Measurement Data — Supplement 1 to the "Guide to the Expression of Uncertainty in Measurement" — Propagation of Distributions Using a Monte Carlo Method, Joint Committee for Guides in Metrology, Sèvres, France, 2008.
[9] J. Sander, R. Kumme, Comparison of force measuring devices with static and continuous loading, Measurement: Sensors 18 (2021), https://doi.org/10.1016/j.measen.2021.100241.
[10] P. Rizza, M. Murgia, A. Prato, C. Origlia, A. Germak, Determination of sensitivity coefficients and their uncertainties in Rockwell hardness measurement: a Monte Carlo method for multiple linear regression, Metrologia 60 (1) (2022), https://doi.org/10.1088/1681-7575/aca334.
[11] A. Prato, F. Mazzoleni, G. D'Emilia, A. Gaspari, E. Natale, A. Schiavi, Metrological traceability of a digital 3-axis MEMS accelerometers sensor network, Measurement 184 (2021), https://doi.org/10.1016/j.measurement.2021.109925.
[12] N. Vlajic, A. Chijioke, Traceable dynamic calibration of force transducers by primary means, Metrologia 53 (S136) (2016), https://doi.org/10.1088/0026-1394/53/4/S136.
[13] ISO 4965-1, Metallic Materials — Dynamic Force Calibration for Uniaxial Fatigue Testing — Part 1: Testing Systems, 2012.

Andrea Prato[a,*], Alessio Improta[b], Michele Di Lernia[b], Salvatore Nobile[b], Alessio Facello[a], Fabrizio Mazzoleni[a], Alessandro Germak[a], Alessandro Schiavi[a]
[a] *INRiM – Istituto Nazionale di Ricerca Metrologica, Torino, Italy*
[b] *Politecnico di Torino, Torino, Italy*

[*] Corresponding author.
*E-mail addresses:* a.prato@inrim.it (A. Prato), alessio.improta@studenti.polito.it (A. Improta), michele.dilernia@studenti.polito.it (M. Di Lernia), salvatore.nobile@studenti.polito.it (S. Nobile), a.facello@inrim.it (A. Facello), f.mazzoleni@inrim.it (F. Mazzoleni), a.germak@inrim.it (A. Germak), a.schiavi@inrim.it (A. Schiavi).